

THE NUMERICAL SOLUTION OF SHALLOW WATER EQUATION BY MOVING MESH METHODS

SUYEON SHIN* AND WOONJAE HWANG**

ABSTRACT. This paper presents a moving mesh method for solving the hyperbolic conservation laws. Moving mesh method consists of two independent parts: PDE evolution and mesh- redistribution. We compute numerical solution of shallow water equation by using moving mesh methods. In comparison with computations on a fixed grid, the moving mesh method appears more accurate resolution of discontinuities.

1. Introduction

The moving mesh methods have been used for solving differential equations that involve singular solution. It gives an improvement in accuracy by moving mesh points that they are concentrate in regions of larger solution variations. Because of this advantage, many useful schemes have been applied on moving grids in recent years.

Several moving mesh techniques have been introduced, in which one of the most advocated methods is the one based on solving elliptic PDEs first proposed by Winslow [25]. Harten and Hyman [6] began the earliest study in this direction, by moving the grid along the characteristic direction to increase the accuracy of solution. After their work, many other moving mesh methods have been proposed. Salari and Steinberg [13] developed a FCT method on a moving grid based on adaptive grid generation algorithms. The moving mesh method based on harmonic

Received June 13, 2012; Accepted June 28, 2012.

2010 Mathematics Subject Classification: Primary 65M50, 76M12; Secondary 35L65.

Key words and phrases: moving mesh, shallow water equation, finite volume methods, conservation laws,

Correspondence should be addressed to Woonjae Hwang, woonjae@korea.ac.kr.

**Supported by Basic Science Research Program through the National Research Foundation of Korea(NRF) funded by the Ministry of Education, Science and Technology(Grant No. 2011-0027131).

mapping was suggested by Dvinsky [4]. His method can be viewed as a generalization and extension of Winslow's method. Motivated by the work of Dvinsky, a moving mesh finite element strategy based on harmonic mapping was proposed and studied by the Li et al. [9, 10]. The moving mesh PDEs were studied by Russell et al. [7, 12, 16], and Li and Petzold [11]. In recent years, there are many works about moving mesh methods [1, 2, 3, 14, 15, 19, 20, 21, 22, 23, 24]. Adaptive mesh method consists of two independent parts [9, 19]: a mesh- redistribution algorithm and a solution algorithm. The first part is an iteration procedure. Meshes are redistributed by an equidistribution principle. For the resulting elliptic, adaptive mesh PDEs, a Gauss-Seidel type iteration method is used. The underlying numerical solution on the new grids are updated by a conservative-interpolation formula. The second part will be independent of the first one, and it can be any of the standard codes for solving the given PDEs.

The organization of this paper is as follows. In Section 2, the moving mesh method is briefly described. Numerical experiments of the one-dimensional hyperbolic conservation laws are provided in Section 3.

2. Moving mesh method

In Tang and Tang [19, 24], the basic idea of the moving mesh method can be summarized by two independent parts: mesh-redistribution and PDE evolution.

2.1. Mesh-redistribution based on Gauss-Jacobi iteration

Meshes are redistributed by an equidistribution principle. The mesh-redistribution equation is

$$(2.1) \quad (wx_\xi)_\xi = 0, 0 < \xi < 1$$

where the function w is called monitor function [16, 17], which designed specifically to resolve discontinuous solutions. To solve the mesh redistribution equation (2.1), the following Gauss-Jacobi type iteration can be used:

$$(2.2) \quad w(u_{j+\frac{1}{2}})(x_{j+1} - \tilde{x}_j) - w(u_{j-\frac{1}{2}})(\tilde{x}_j - x_{j-1}) = 0,$$

and then the underlying numerical solution on the new grids $\{\tilde{x}_{j+\frac{1}{2}}\}$ are updated by a conservative-interpolation formula. The conservative-interpolation formula is following:

$$(2.3) \quad \Delta \tilde{x}_{j+\frac{1}{2}} \tilde{u}_{j+\frac{1}{2}} = \Delta x_{j+\frac{1}{2}} u_{j+\frac{1}{2}} - ((cu)_{j+1} - (cu)_j),$$

where $\Delta\tilde{x}_{j+\frac{1}{2}} = \tilde{x}_{j+1} - \tilde{x}_j$. The linear flux cu in (2.3) is approximated by second-order numerical flux. The second-order numerical flux is defined by

$$(2.4) \quad (cu)_j = \frac{c_j}{2}(u_j^+ + u_j^-) - \frac{|c_j|}{2}(u_j^+ - u_j^-).$$

The wave speed c_j above is defined by $c_j = x_j - \tilde{x}_j$. In (2.4), $u_j^{n,\pm}$ are defined by

$$(2.5) \quad u_j^{n,\pm} = u_{j\pm\frac{1}{2}}^n + \frac{1}{2}(x_j - x_{j\pm 1})\tilde{S}_{j\pm\frac{1}{2}},$$

where $\tilde{S}_{j+\frac{1}{2}}$ is an approximation of the slope u_x at $x_{j+\frac{1}{2}}$. $\tilde{S}_{j+\frac{1}{2}}$ is defined by

$$(2.6) \quad \tilde{S}_{j+\frac{1}{2}} = (\text{sign}(\tilde{S}_{j+\frac{1}{2}}^+) + \text{sign}(\tilde{S}_{j+\frac{1}{2}}^-)) \frac{|\tilde{S}_{j+\frac{1}{2}}^+ \tilde{S}_{j+\frac{1}{2}}^-|}{|\tilde{S}_{j+\frac{1}{2}}^+| + |\tilde{S}_{j+\frac{1}{2}}^-|},$$

with

$$(2.7) \quad \tilde{S}_{j+\frac{1}{2}}^+ = \frac{u_{j+\frac{3}{2}}^n - u_{j+\frac{1}{2}}^n}{x_{j+\frac{3}{2}} - x_{j+\frac{1}{2}}}, \quad \tilde{S}_{j+\frac{1}{2}}^- = \frac{u_{j+\frac{1}{2}}^n - u_{j-\frac{1}{2}}^n}{x_{j+\frac{1}{2}} - x_{j-\frac{1}{2}}}.$$

The equation (2.5)~(2.7) are the MUSCL(monotone upstream-centered scheme for conservation laws)-typed finite volume method. The new grid procedure by the Gauss-Jacobi type iteration and the updated solution procedure using the conservative-interpolation are repeated for a fixed number of iterations or untill $\|x^{[v+1]} - x^{[v]}\| \leq \epsilon$.

2.2. PDE evolution

The mesh redistribution is based on an iteration procedure and the PDE evolution is independent of the first part. It can be solved by using any high resolution finite volume methods. In this paper, a second-order finite volume scheme with a numerical flux is the Lax-Friedrichs flux:

$$(2.8) \quad \hat{f}(a, b) = \frac{1}{2}[f(a) + f(b) - \max_u\{|f_u|\}(b - a)].$$

The details can be found in Tang and Tang [19].

3. Numerical experiments

In this section, we consider the one-dimensional hyperbolic conservation laws

$$(3.1) \quad u_t + f(u)_x = 0, \quad t > 0.$$

As a scalar model, we consider Buckley - Leverett equation. For a system model, we consider the shallow water equation [5, 18]. We consider the Riemann problem for both equations. Some details are the following: the number of Jacobi iterations is 5; the scheme for evolving this equation is a (formally) second-order MUSCL finite volume scheme (with the Lax-Friedrichs flux) together with a second-order Runge-Kutta discretization; the CFL number used is 0.3.

EXAMPLE 3.1. We consider Buckley-Leverett problem [8],

$$(3.2) \quad u_t + f(u)_x = 0, \quad f(u) = \frac{u^2}{u^2 + a(1-u)^2}, \quad a = 0.5.$$

The initial data are

$$u(x, 0) = \begin{cases} 1 & \text{if } x < 0 \\ 0 & \text{if } x > 0. \end{cases}$$

This may be used to model gas and oil in a reservoir, where u is the fluid saturation(water). This flux is nonconvex with a single inflection point. The characteristic speed is $f'(u) = \frac{2au(1-u)}{[u^2+a(1-u)^2]^2}$. By following characteristics, we can construct the triple-valued solution. By the

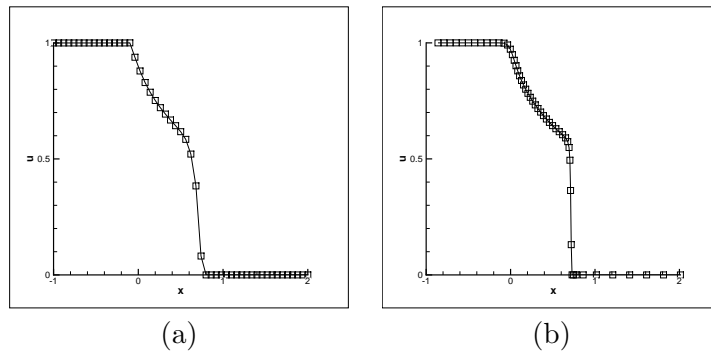


FIGURE 1. (a) Numerical solutions by MUSCL, (b) Numerical solutions by MUSCL with MMM ($J=50$).

equal-area rule, this triple-valued solution replaced a shock. Thus Riemann solution involves both a shock and a rarefaction wave and is called a compound wave.

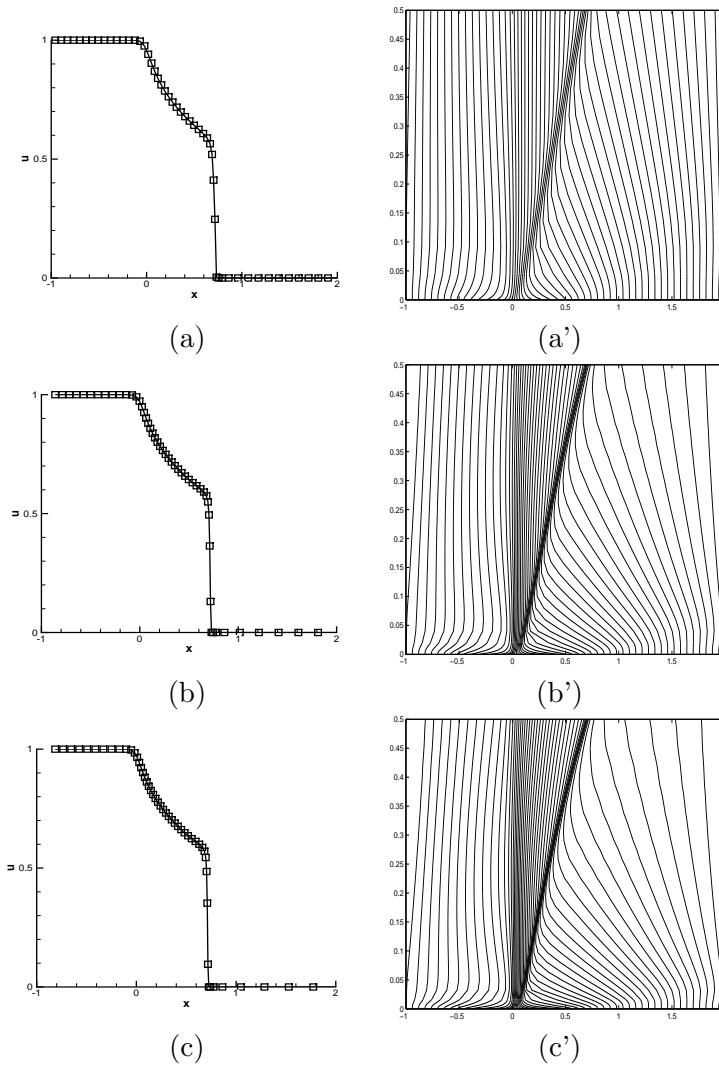


FIGURE 2. (a),(b), and (c) show numerical solutions by MUSCL with MMM of monitor parameter 1, 10, and 20, respectively. (a'),(b'), and (c') show mesh trajectories of monitor parameter 1, 10, and 20, respectively. ($J=50$)

Figure 1 (a) and (b) show the numerical solutions at $t = 0.5$ for uniform grid and nonuniform grid, respectively obtained with the number of grids $J = 50$. The monitor function used in the computation is

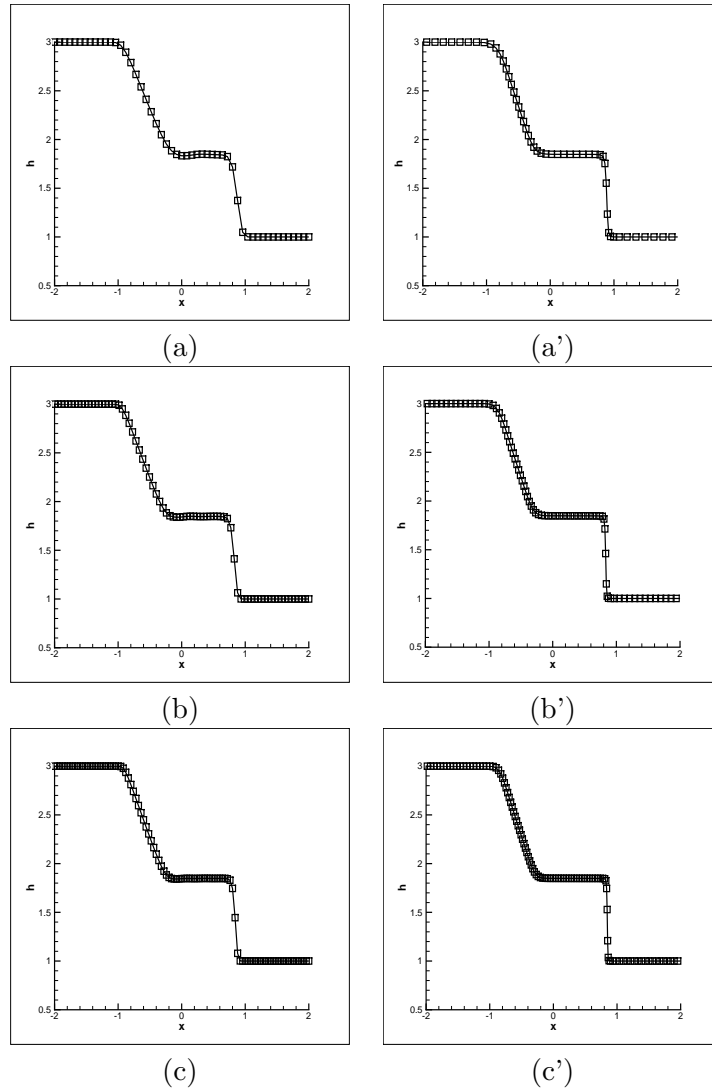


FIGURE 3. Height: (a),(b), and (c) show numerical solutions by MUSCL of $J = 50, 75,$ and $100,$ respectively. (a'),(b'), and (c') show numerical solutions by MUSCL with MMM of $J = 50, 75,$ and $100,$ respectively.

$w = \sqrt{1 + 10|u_\xi|^2}$. In this example, the monitor function is taken as $w = \sqrt{1 + \beta|u_\xi|^2}$, $\beta > 0$ where several values of β are used. In Figure 2, the numerical solution and mesh trajectories with three different

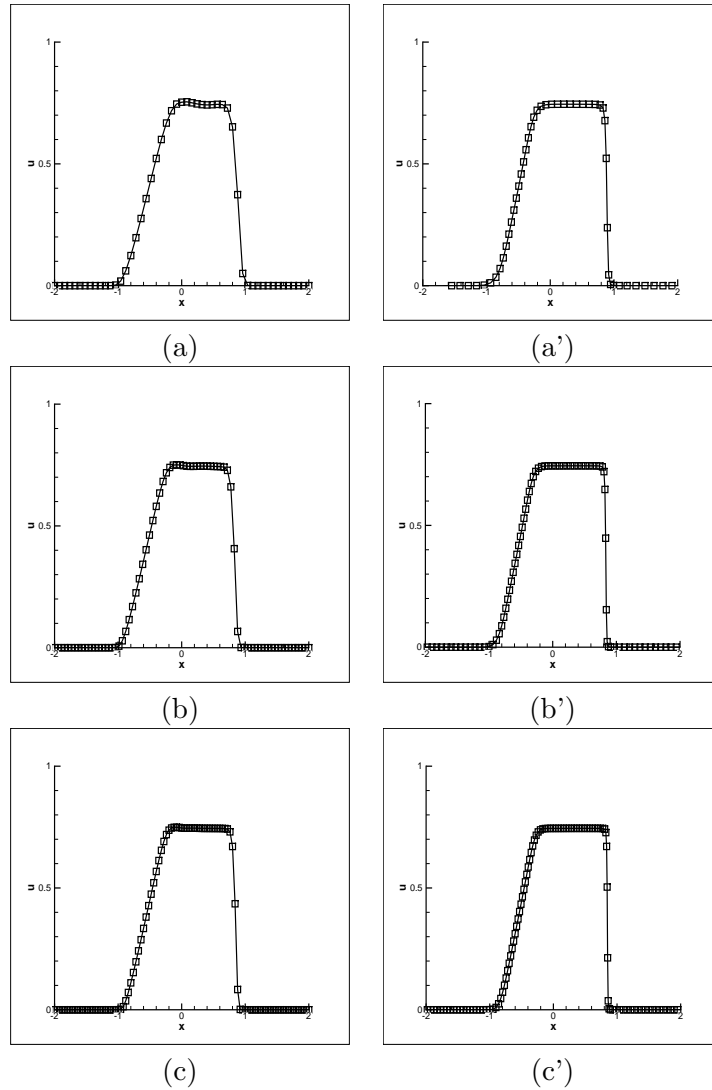
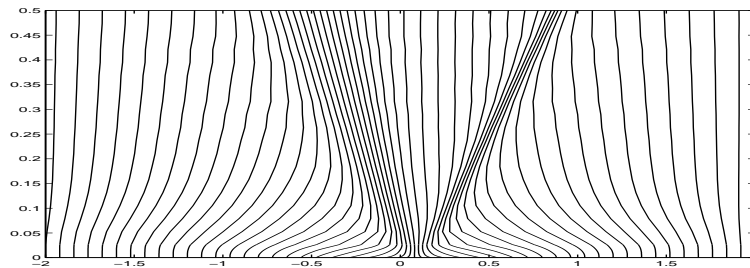
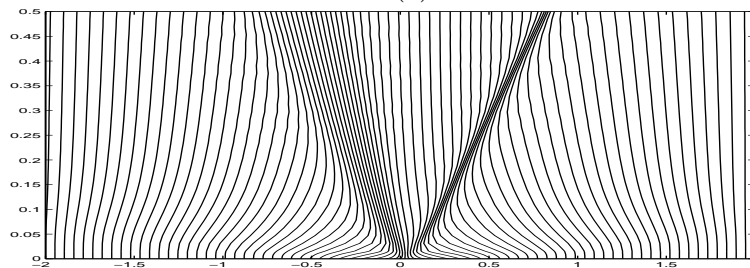


FIGURE 4. Velocity: (a),(b), and (c) show numerical solutions by MUSCL of $J = 50, 75,$ and $100,$ respectively. (a'),(b'), and (c') show numerical solutions by MUSCL with MMM of $J = 50, 75,$ and $100,$ respectively.

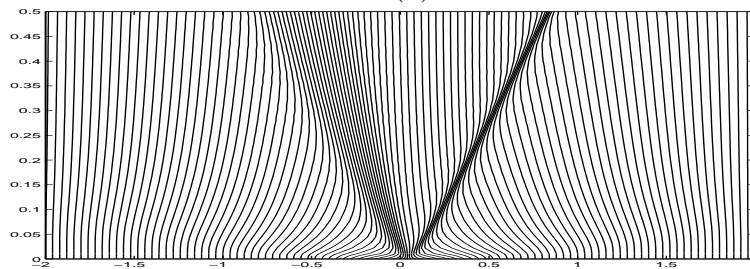
monitor functions ($\beta = 1, 10, 20$) are plotted. It is observed that the grid distributions seem more reasonable, with more points where the value of curvature is large. However, we avoid clustering too many points in the neighborhood of the discontinuities. Thus parameter $\beta = 10$ of monitor function is efficient choice. Obviously, the study on how to choose the monitor constants seems very useful. In principle, the monitor function w can be any appropriately chosen measure of the numerical error in the solution of the PDE. At points where the error is large, w should also be large so that mesh points will tend to concentrate in those areas where higher resolution is needed.



(a)



(b)



(c)

FIGURE 5. (a), (b), and (c) show mesh trajectories for $J = 50, 75,$ and $100,$ respectively.

EXAMPLE 3.2. We apply moving mesh algorithm to the one-dimensional shallow water equations,

$$\begin{pmatrix} h \\ hu \end{pmatrix}_t + \begin{pmatrix} hu \\ hu^2 + \frac{1}{2}gh^2 \end{pmatrix}_x = 0$$

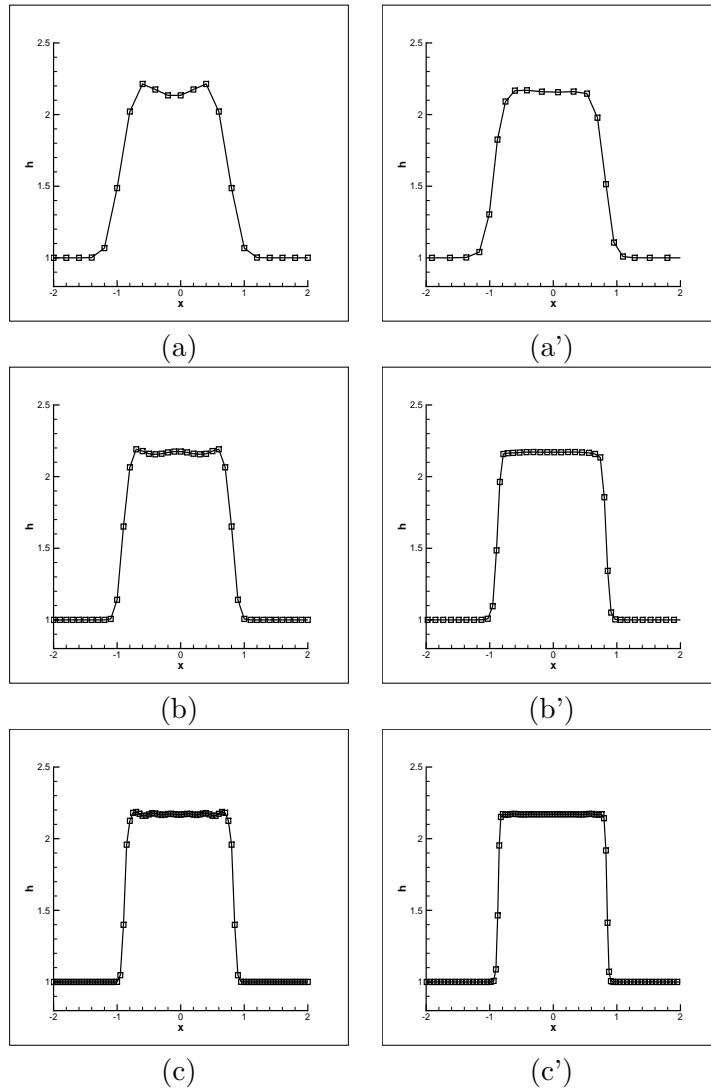


FIGURE 6. Height: (a),(b), and (c) show numerical solutions by MUSCL of $J = 20, 40,$ and $80,$ respectively. (a'),(b'), and (c') show numerical solutions by MUSCL with MMM of $J = 20, 40,$ and $80,$ respectively.

where h , u and g are height, velocity and gravitational constant, respectively. Consider the shallow water equation with the piecewise-constant

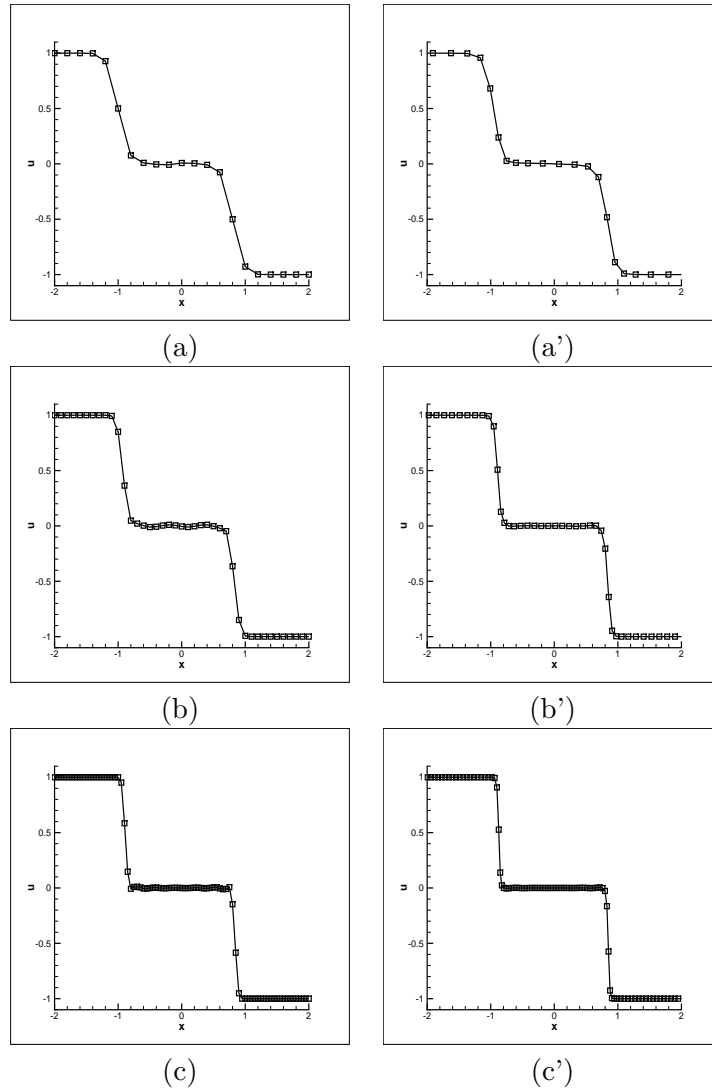


FIGURE 7. Velocity: (a),(b), and (c) show numerical solutions by MUSCL of $J = 20, 40$, and 80 , respectively. (a'),(b'), and (c') show numerical solutions by MUSCL with MMM of $J = 20, 40$, and 80 , respectively.

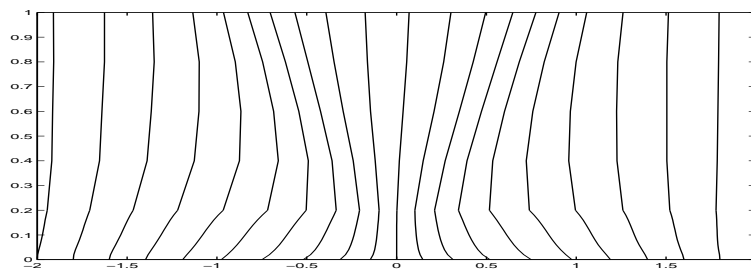
initial data

$$h(x, 0) = \begin{cases} 3 & \text{if } x < 0 \\ 1 & \text{if } x > 0, \end{cases}$$

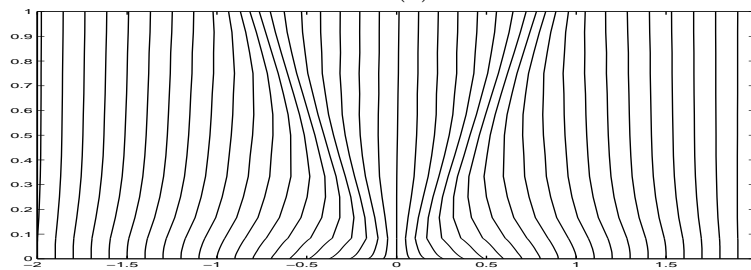
$$u(x, 0) = 0.$$

This is special case of the Riemann problem in which $u_l = u_r = 0$, and is called the dam-break problem because it models what happens if a dam separating two levels of water bursts at time $t = 0$.

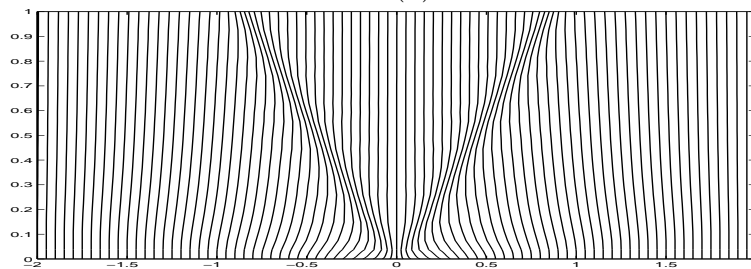
Figures 3 and 4 show the solutions of height and velocity, respectively at $t = 0.5$ for uniform and nonuniform grid, obtained with $J = 50$,



(a)



(b)



(c)

FIGURE 8. (a), (b), and (c) show mesh trajectories for $J = 50, 75$, and 100 , respectively.

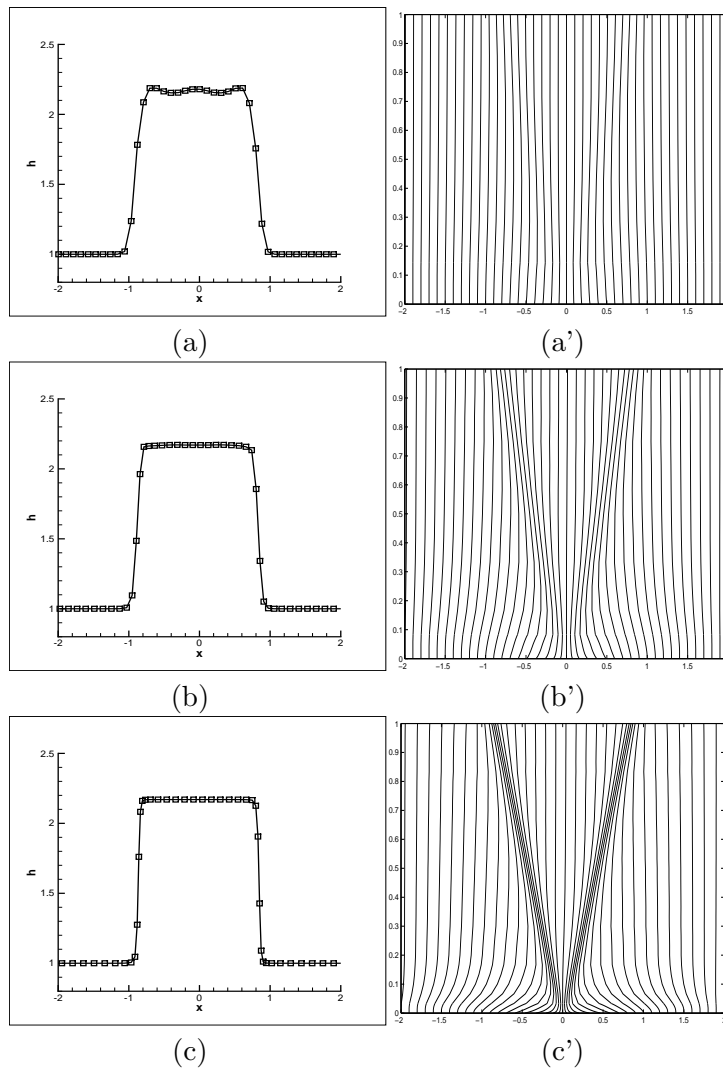


FIGURE 9. Height: (a),(b), and (c) show numerical solutions by MUSCL with MMM of monitor parameter 1, 10, and 100 respectively. (a'),(b'), and (c') show mesh trajectories of monitor parameter 1, 10, and 100, respectively. ($J=40$)

$J = 75$, and $J = 100$. Figure 5 shows the trajectories of the grid points at $t=0.5$, obtained with $J=50$, $J=75$, and $J=100$. In this example, the monitor function used in the computation is $w = \sqrt{1 + 100(\frac{|h_\xi|}{\max_\xi |h_\xi|})^2}$.

EXAMPLE 3.3. Consider the shallow water equation with the piecewise-constant initial data

$$h(x, 0) = 1,$$

$$u(x, 0) = \begin{cases} 1 & \text{if } x < 0 \\ -1 & \text{if } x > 0. \end{cases}$$

The solution is symmetric in x with $h(-x, t) = h(x, t)$ and $u(-x, t) = -u(x, t)$ at all times. A shock waves moves in direction, bringing the fluid to rest, since the middle state must have $u_m = 0$ by symmetry.

Figures 6 and 7 show the solutions of height and velocity, respectively at $t = 1$ for uniform and nonuniform grid, obtained with $J = 20$, $J = 40$, and $J = 80$. Figure 8 shows the trajectories of the grid points at $t=1$, obtained with $J=20$, $J=40$, and $J=80$. In this example, the monitor function used in the computation is $w = \sqrt{1 + 10(\frac{|u_\xi|}{\max_\xi |u_\xi|})^2}$. In this example, the monitor function is taken as $w = \sqrt{1 + \beta(\frac{|u_\xi|}{\max_\xi |u_\xi|})^2}$, $\beta > 0$ where several values of β are used. In Figure 9, the mesh trajectories and numerical solution with three different monitor functions ($\beta = 1, 10, 100$) are plotted.

References

- [1] B. N. Azarenok, S. A. Ivanenko, and T. Tang, *Adaptive mesh redistribution method based on Godunov's scheme*, Communications in Mathematical Sciences **1** (2003), 152-179.
- [2] B. N. Azarenok and T. Tang, *Second-order Godunov-type scheme for reactive flow calculations on moving meshes*, Journal of Computational Physics **206** (2005), 48-80.
- [3] Y. Di, R. Li, T. Tang and P.W. Zhang, *Moving mesh finite element methods for the incompressible Navier-Stokes equations*, AMJ. Sci. Comput. **26** (2005), 1036-1056.
- [4] A. S. Dvinsky, *Adaptive grid generation from harmonic maps on Riemannian manifolds*, Journal of Computational Physics, **95** (1991), 450-476.
- [5] J. Felcman and L. Kadrnka, *On a Moving Mesh Method Applied to the Shallow Water Equations*, Numerical Analysis and Applied Mathematics, International Conference **1** (2010), 195-198.
- [6] A. Harten, J. M. Hyman, *Self-adjusting grid methods for one-dimensional hyperbolic conservation laws*, Journal of Computational Physics **50** (1983), 235-269.

- [7] W. Huang, Y. Ren and R. D. Russell, *Moving mesh methods based on moving mesh partial differential equations*, Journal of Computational Physics **113** (1994), 279-290.
- [8] R. J. Leveque, *Finite volume methods for hyperbolic problems*, Cambridge University Press, Cambridge, 2002.
- [9] R. Li, T. Tang and P. Zhang, *Moving mesh methods in multiple dimensions based on harmonic maps*, Journal of Computational Physics **170** (2001), 562-588.
- [10] R. Li, T. Tang and P. Zhang, *A moving mesh finite element algorithm for singular problems in two and three space dimensions*, Journal of Computational Physics **177** (2002), 365-393.
- [11] S. Li, L. Petzold, *Moving mesh methods with upwinding schemes for time-dependent PDEs*, Journal of Computational Physics **131** (1997), 368-377.
- [12] Y. Ren, R. Ren and Russell, *Moving mesh partial differential equations(MMPDES) based on the equidistribution principle*, SIAM Journal on Numerical Analysis **31** (1994), 709-730.
- [13] K. Saleri, S. Steinberg, *Flux-corrected transport in a moving grid*, Journal of Computational Physics **111** (1994), 24-32.
- [14] S. Shin, *Adaptive mesh method for conservation laws*, Master thesis, Korea University, Seoul, 2006.
- [15] S. Shin and W. Hwang, *Numerical solution of burgers' equation by moving mesh methods*, Proceedings of the National Institute for Mathematical Sciences **1** (2006), 100-103.
- [16] J. M. Stockie, J. A. Mackenzie, and R. D. Russell, *A moving mesh method for one-dimensional hyperbolic conservation laws*, SIAM Journal on Scientific Computing **22** (2001), 1791-1813.
- [17] Z. Tan, Z. Zhang, Y. Huang, and T. Tang, *Moving mesh methods with locally varying time steps*, Journal of Computational Physics **200** (2004), 347-367.
- [18] H. Tang, *Solution of the shallow-water equations using an adaptive moving mesh method*, International Journal for Numerical Methods in Fluids **44** (2004), 789-810.
- [19] H. Tang and T. Tang, *Adaptive mesh methods for one-and two-dimensional hyperbolic conservation laws*, SIAM Journal on Numerical Analysis **41** (2003), 487-515.
- [20] H. Z. Tang and T. Tang, *Multi-dimensional moving mesh methods for shock computations*, Inter. Conf. on Sci. Comput. and PDEs, on the Occasion of S. Osher's 60th birthday, Dec. 12-15, 2002, Hongkong. Contemporary Mathematics **330** (2003), 169-183.
- [21] H. Z. Tang, T. Tang, P. Zhang, *An adaptive mesh redistribution method for nonlinear Hamilton-Jacobi equations in two- and three-dimensions*, Journal of Computational Physics **188** (2003), 543-572.
- [22] T. Tang, *Moving mesh methods for computational fluid dynamics*, Contemporary Mathematics **383** (2005), 141-173.
- [23] P. A. Zegeling, W. D. de Boer, and H. Z. Tang, *Robust and efficient adaptive moving mesh solution of the 2-D Euler equations*, Contemporary Mathematics **383** (2005), 375-386.

- [24] Z. Zhang and T. Tang, *An adaptive mesh redistribution algorithm for convection-dominated problems*, Communications on pure and Applied Analysis **1** (2002), 341-357.
- [25] A. Winslow, *Numerical solution of the quasi-linear Poisson equation in a nonuniform triangle mesh*, Journal of Computational Physics **1** (1967), 149-172.

*

Department of Mathematics
Korea University
Seoul 136-701, Republic of Korea
E-mail: angelic52@korea.ac.kr

**

Department of Information and Mathematics
Korea University
Jochiwon 339-700, Republic of Korea
E-mail: woonjae@korea.ac.kr